Journal of Wind Engineering and Industrial Aerodynamics, 8 (1981) 93—104

SHELTER BEHIND TWO-DIMENSIONAL SOLID AND POROUS FENCES*

M.D.A.E.S. PERERA

Building Research Station, Garston, Herts (Gt. Britain)

Summary

Using a pulsed-wire anemometer, extensive measurements have been made in the wakes of two-dimensional solid and porous fences immersed in the constant-stress region of a simulated rural atmospheric boundary-layer. The porosity (ratio of open to total area) of the perforated fences ranged from 0.0 to 0.5 and each porosity was modelled using three forms of openings, i.e. vertical slats, horizontal slats and circular holes.

Comparative measurements made using the more conventional hot-wire anemometer are given. The results show the superiority of the pulsed-wire anemometer in correctly measuring the highly turbulent and sometimes recirculating wake flows. This indicates that previously reported experiments may be in considerable error.

Results from the present experiment are given in the form of dimensionless mean and turbulence velocity profiles. In addition, contour plots of shelter parameters behind the fences are given for comfort and shelter analyses.

Downstream of the re-attachment region, velocity deficits and excess shear and normal stress perturbations (quantities useful in shelter analyses) are plotted in a self-preserving form and simple equations that fit the experimental points are given.

Power spectra measured in the presence of the solid fence are given and the structure of the turbulent wake deduced from these is discussed.

1. Introduction

Windbreaks and shelterbelts have played and continue to play a significant role in protecting man and his micro-environment. It is therefore of considerable interest to know the "correct" characteristics of any particular shelter device in order to obtain optimum performance for any particular application.

At present, despite a considerable amount of full-scale and model research, there are no firm guidelines on the performance of shelter devices. In 1964, van Eimern et al. [1] reviewed the literature then available but could draw only a few general conclusions. A survey of the literature published since then has shown that the picture is still unclear. One major reason for this may be the inability of conventional wind-velocity measuring instruments, such as the hot-wire anemometer (HWA), to measure correctly in the highly turbulent and usually recirculating wake-flow region behind these shelter devices.

*Paper presented at the 4th Colloquium on Industrial Aerodynamics (Building Aerodynamics), Aachen, June 19—20, 1980.

To resolve these difficulties, the wake flows behind solid and porous fences were measured with a pulsed-wire anemometer (PWA). The PWA, unlike the HWA, does not rectify positive- and negative-going velocities but can discriminate between them. Again, unlike the HWA, it can be used to measure highly turbulent flows [2].

Fences with porosities ϕ (ratio of open to total area) ranging from 0.0 to 0.5 were tested in the constant-stress region of a simulated rural atmospheric boundary-layer. For each value of ϕ, three fences consisting entirely of either horizontal slats, vertical slats or circular holes were tested.

2. Experimental

Measurements were made in an open-circuit type wind tunnel with a 2.00 × 1.25 m working section. Partial depth-simulation of a rural atmospheric boundary-layer was achieved by using a modified biplanar grid and a saw-tooth barrier placed near the downstream end of the tunnel contraction. The flow was then allowed to develop over a 5-m fetch of gravel.

The height h of each fence was set to a value of 40 mm. In order to achieve two-dimensionality of the centre-line wake flow, their lengths were set to 1 m. Porosities of the fences were modelled either with circular holes (minimum diameter 8 mm) or horizontal or vertical slits (minimum width 5 mm). The minimum dimensions were set in order to satisfy Reynolds-number criteria for turbulent flow through these openings.

The measuring instruments could be traversed to any point in the flow field, under computer control. The acquisition and analysis of data was done with an on-line minicomputer. The digital form of the output of the PWA limited the sampling rate to ~25 samples/s whereas the analogue output of the HWA enabled a sampling rate of 1024 samples/s.

The fences were immersed in a simulated atmospheric boundary-layer ~250 mm deep. The friction velocity u_* was estimated as 0.57 m s^{-1} and the variation of $(\overline{-u'w'})^{1/2}$ was constant to within 10% of u_* throughout the layer. The mean-velocity profile satisfied the logarithmic law of the wall:

$$\bar{u}(z)/u_* = (1/k)\cdot\ln((z-d)/z_0)$$

where $\bar{u}(z)$ is the variation of the longitudinal component of wind with height z. The zero displacement d and roughness length z_0 were 1.6 and 0.3586 mm respectively; k is the von Karman constant and has the value 0.41.

The power spectrum of the longitudinal component of turbulence, u', in the undisturbed simulated boundary layer, measured at height h, satisfied the von Karman interpolation formula

$$n\cdot S(n)/\overline{u'^2} = 0.115\,\tilde{n}/(0.014 + \tilde{n}^2)^{5/6}$$

where $\tilde{n}$ (= $0.1456\,n/n_p$) is the modified frequency and n_p is the frequency at which the measured spectrum peaks. The integral length-scale derived from the above formula and substituted into an equation giving its functional

dependence on z_0 [3] gave a length-scale factor of 1:200 for the simulation. These turbulence measurements together with the mean-velocity profiles confirmed that the simulated boundary layer satisfied parameters relating to a flow over a moderately rough terrain containing short grass or crops [4].

3. Results

3.1 Comparison between HWA and PWA measurements

In order to compare the results from the PWA with those from an HWA, measurements were made in both the windward and leeward regions of the solid fence. Figures 1(a) and 1(b) show representative profiles of the normalised mean velocity $\bar{u}_N$ $(= \bar{u}(z)/\bar{u}_R(h))$, and turbulence intensity I $(= \bar{u}(z)/\bar{u}_R(h))$, respectively, where the reference velocity $\bar{u}_R(h)$ is measured in the absence of the fence. In each of these figures, the first profile in each series is the reference profile, i.e. that at the fence station without the fence in place.

Figures 1(a) and 1(b) clearly show that there are discrepancies between the two sets of measurements in both the leeward and windward regions of the flow. The velocity profiles indicate that the HWA results are consistently higher and that within the recirculating zone, the velocities are positive and do not, unlike the PWA results, indicate the reversing flow. For the intensity profiles, however, the differences are not qualitative but quantitative. Profiles at any station are of similar form and the highly turbulent shear layer emanating from the top of the fence can be seen in both sets of measurements. However, as for the mean-velocity profiles, noticeable differences exist even as far downstream as $22h$.

3.2 Effect of construction form

Figure 2 shows the distribution of normalised mean velocity downstream of the fences with porosity 0.1, the measurements being made at a height of $h/2$. Apart from a very small region windward of the fence (influenced by the local structure of the flow through the openings), the results are virtually independent of the form of fence construction. This observation is also true for other combinations of measuring heights and fence porosities. As a consequence, the remainder of this paper will be confined to measurements made for the horizontal-slot fences.

3.3 Velocity and turbulence intensity profiles

Profiles of normalised longitudinal velocity are shown in Fig. 3. For clarity, only a few representative profiles for fences with ϕ = 0.0, 0.1 and 0.3 are shown at selected measuring stations. They show that as porosity, and hence the bleed flow, increases, the recirculating bubble decreases in size and moves downstream. A similar observation was made by Castro [5] from measurements behind porous plates immersed totally in a smooth flow. The recirculating bubble exists here only for porosities less than 0.3.

From the velocity profiles it is seen that the wake velocities increase with

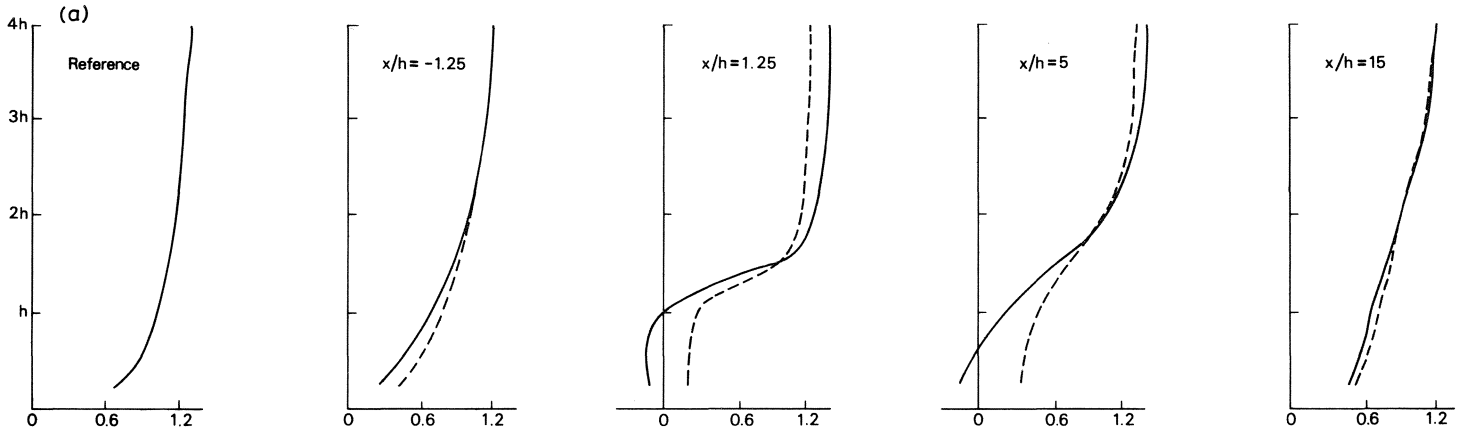

Fig. 1(a). Profiles of normalised mean velocity behind solid fence (measurements: ——, PWA; - - - - -, HWA.

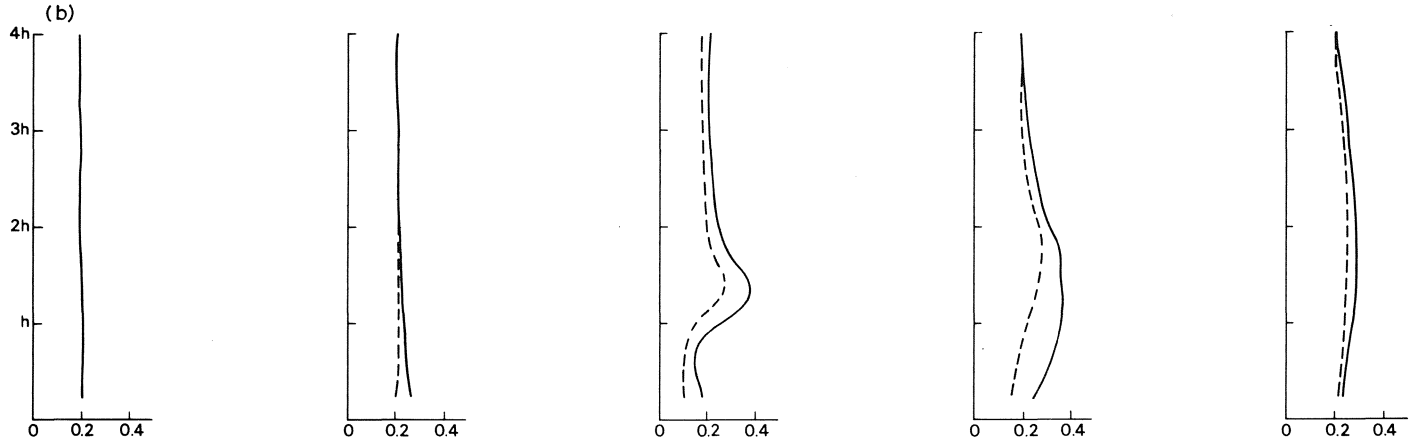

Fig. 1(b). Profiles of longitudinal turbulence intensity behind solid fence (measurements: ——, PWA; - - - - -, HWA).

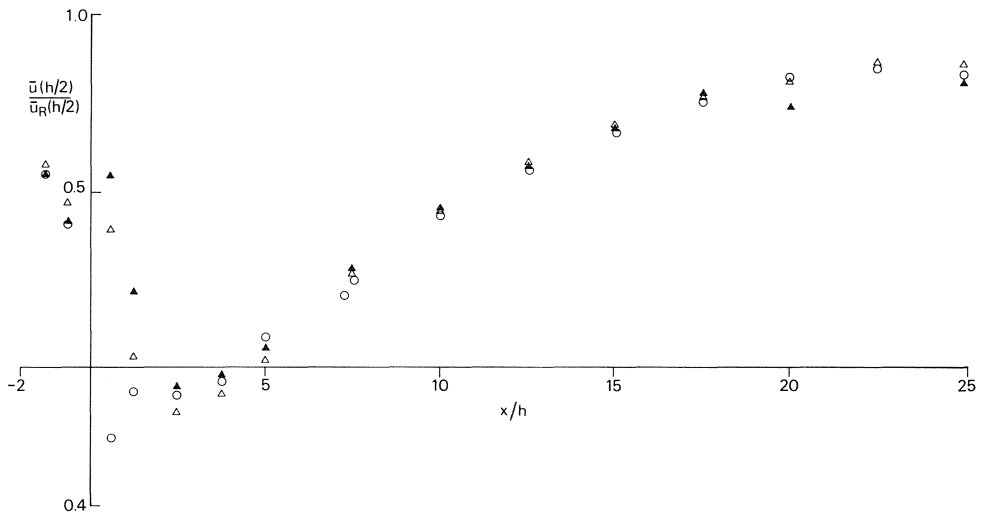

Fig. 2. Normalised mean velocity profiles in the presence of $\phi = 0.1$ fences. Construction: ○, circular; △, vertical; ▲, horizontal.

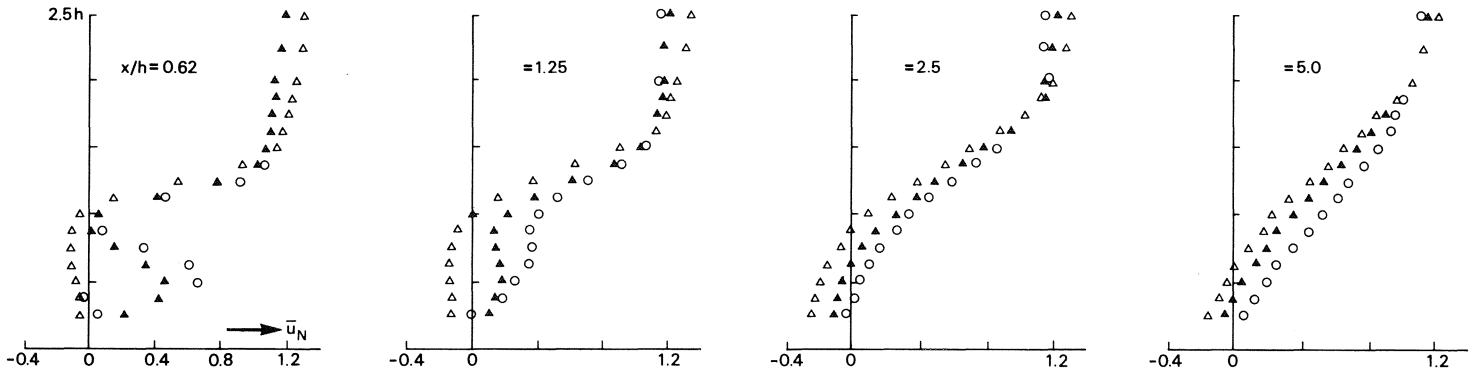

Fig. 3. Normalised longitudinal velocity profiles: △, solid; ▲, $\phi = 0.1$; ○, $\phi = 0.3$.

increasing porosity. In contrast to this, the turbulence intensity decreases with increasing porosity. It must be noted, however, that the solid fence provides a flow of very low turbulence in the near-wake zone.

3.4 Shelter parameters

On the basis of the above observations, any shelter parameter should take into account both the mean and turbulence properties of the wind. Gandemer [6] has defined such a parameter:

$$\psi = [|\bar{u}(z)| + (\overline{u'^2(z)})^{1/2}]/[\bar{u}_R(z) + (\overline{u'^2_R(z)})^{1/2}]$$

Contour plots of ψ are shown in Fig. 4. It can be seen that, away from the immediate vicinity of the fence, the fence of porosity 0.1 provides the best overall shelter, in contrast with the higher values suggested by previous experimenters. Nearer the fence, the solid fence provides the best shelter. Hence, the designer must consider the area he or she wishes to protect and, using such contour maps, design the fence accordingly.

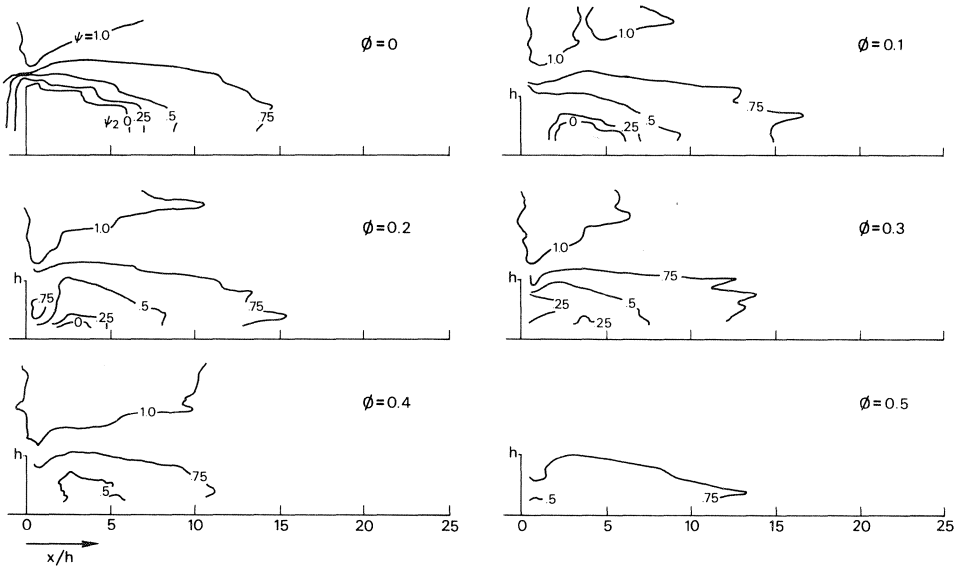

Fig. 4. Contour plots of Gandemeer's shelter parameter ψ behind solid and porous fences.

3.5 Wake velocity defects

The velocity defect $\Delta\bar{u}$ ($= \bar{u}_R(z) - \bar{u}(z)$) in the fence wake is the most useful parameter for practical and theoretical purposes. When a flow is self-preserving, profiles of $\Delta\bar{u}$ may be made to satisfy functional forms by an appropriate choice of length scales. Using non-dimensionalised parameter groupings proposed by Counihan et al. [7], it can be shown that, in the far-

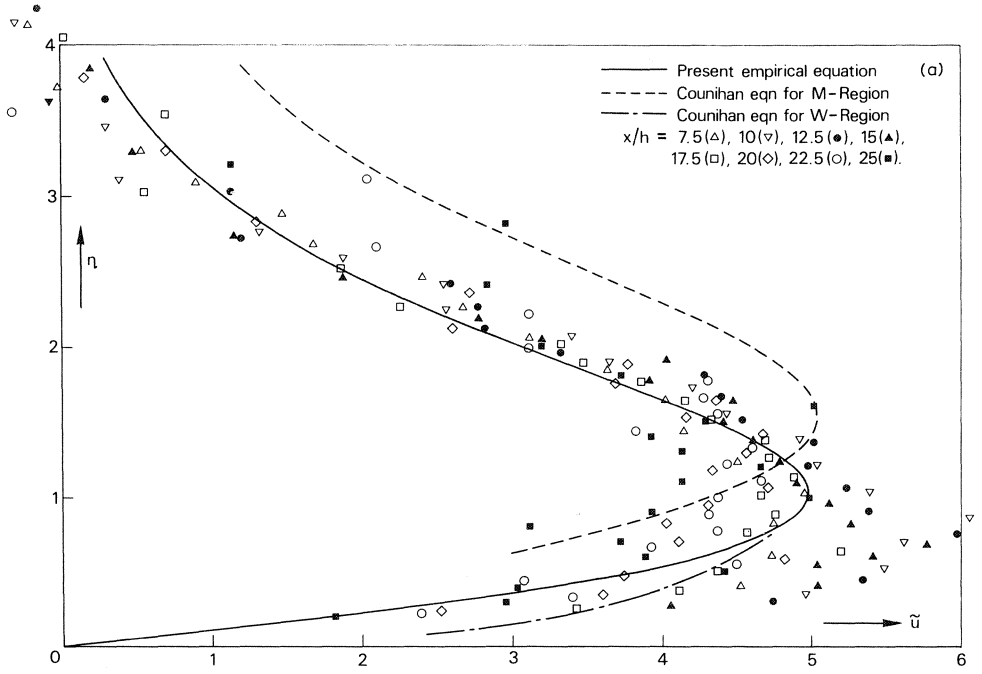

Fig. 5(a). Velocity-deficit profiles behind solid fence.

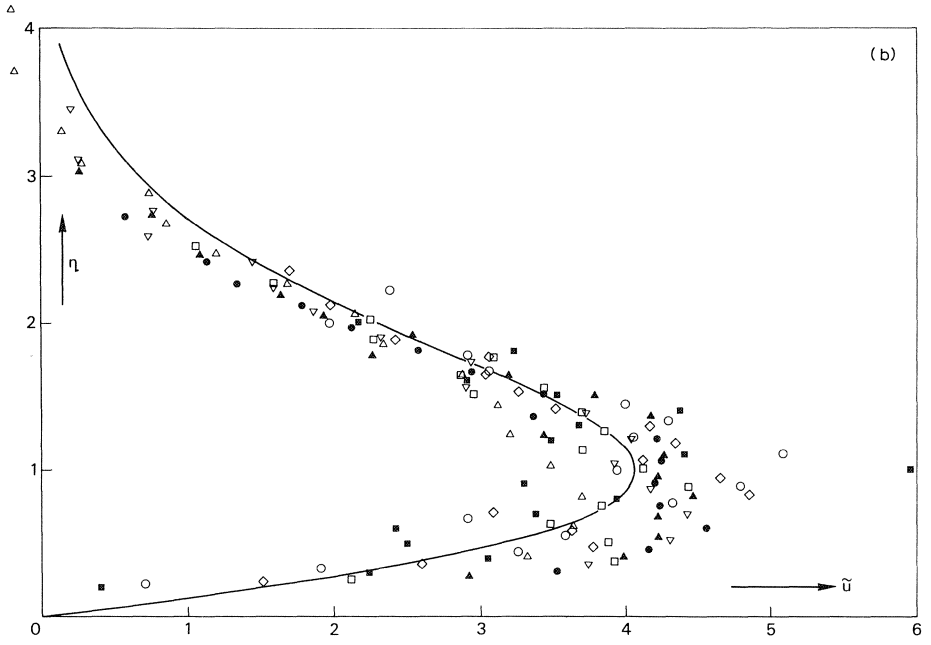

Fig. 5(b). Velocity-deficit profiles behind ϕ = 0.2 fence (for key, see Fig. 5(a)).

wake zone (~7.5 h downstream), such profiles may be represented approximately by the empirical formula

$$\tilde{u} = 9.75\,(1-\phi)\,\eta\cdot\exp(-0.67\eta^{1.5}) \qquad (1)$$

where $\tilde{u} = -[\Delta\bar{u}(z)/\bar{u}_R(h)]\cdot\bar{x}$ and $\eta = [y/(h-d)]\,(1/K\bar{x})^{1/(n+2)}$. Here n is the exponent of the approach velocity profile, $\bar{x} = x/(h-d)$, and $K = 2\,k^2/[\ln(h-d)/Z_0]$ in a constant-stress boundary layer [7].

This equation has been fitted (Fig. 5) to the experimental points for two representative porosities of 0.0 and 0.2. On the plot for the solid fence (Fig. 5(a)), the confluent hypergeometric form proposed by Counihan et al. [7] is shown. Adding to the complexity of this solution, they proposed two forms, one for the wall region and the other for the mixing region [7]. Figures 5(a) and 5(b) show that as well as giving a single, simple, empirical expression to satisfy both regions, eqn. (1) also provides a better fit to the experimental data.

3.6 Excess-stress perturbations

The shear stress perturbations $\Delta(\overline{-u'w'})$ obtained from HWA measurements were plotted in the form $\Delta(\overline{-u'w'})\cdot x^{(3+n)/(2+n)}\bar{u}_R^2(h)$ versus η, as suggested by Counihan et al. [7]. Because the collapse of the experimental points was very poor, the data were re-plotted in the form $\Delta(\overline{-u'w'})\cdot\bar{x}/\bar{u}_R^2(h)$ versus

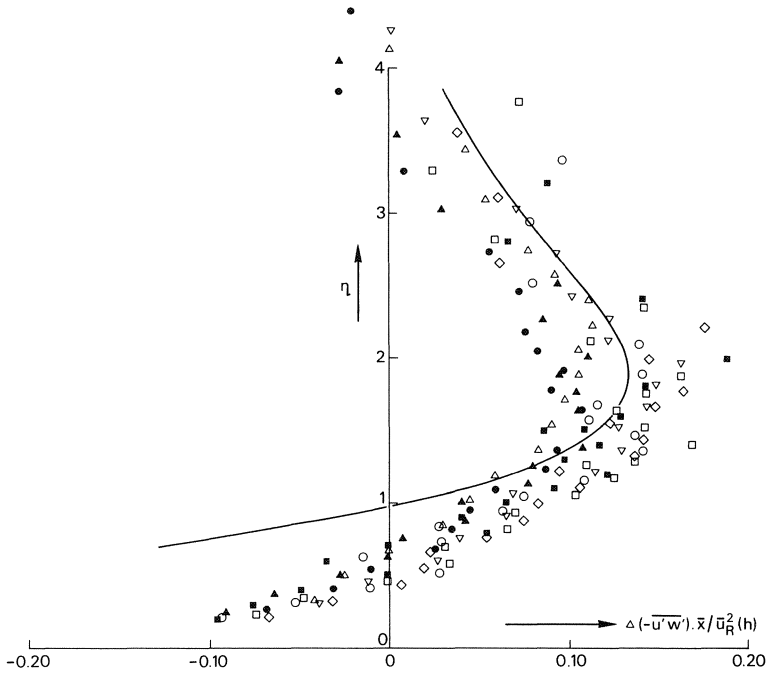

Fig. 6. Excess shear-stress profiles behind solid fence (for key, see Fig. 5(a)).

η. A much better collapse of the data is obtained (Fig. 6), implying that shear-stress perturbations decay as x^{-1}, and not as $x^{-3/2}$ as suggested by Counihan et al. [7]. The —1 exponent for decay compares with that predicted by Townsend [8].

An empirical equation of the form

$$[\Delta(\overline{-u'w'})/\bar{u}_R^2(h)]\cdot\bar{x} = 9.75\,(1-\phi)\cdot K\exp(-0.67\eta^{1.5})\cdot(\eta^{1.5}-1)$$

satisfies the perturbations in the mixing region and predicts the maximum shear-stress excess and its location well.

The normal stress perturbations $\Delta(\overline{u'^2})$ also collapse when the data are plotted in the form $[\Delta\bar{u}'^2/\bar{u}_R^2(h)]\cdot\bar{x}$ versus η. It should be noted that the decay of the stress perturbations as x^{-1} is similar to that obtained from grid-generated turbulence, even though the two flows are dissimilar. An empirical equation

$$\Delta(\bar{u}'^2) = \mu_1\cdot\Delta(\overline{-u'w'})$$

fit the experimental points well (Fig. 7). From the PWA measurements, the constant μ_1 can be represented by

$$\mu_1 = 4.23 - 6.67\phi$$

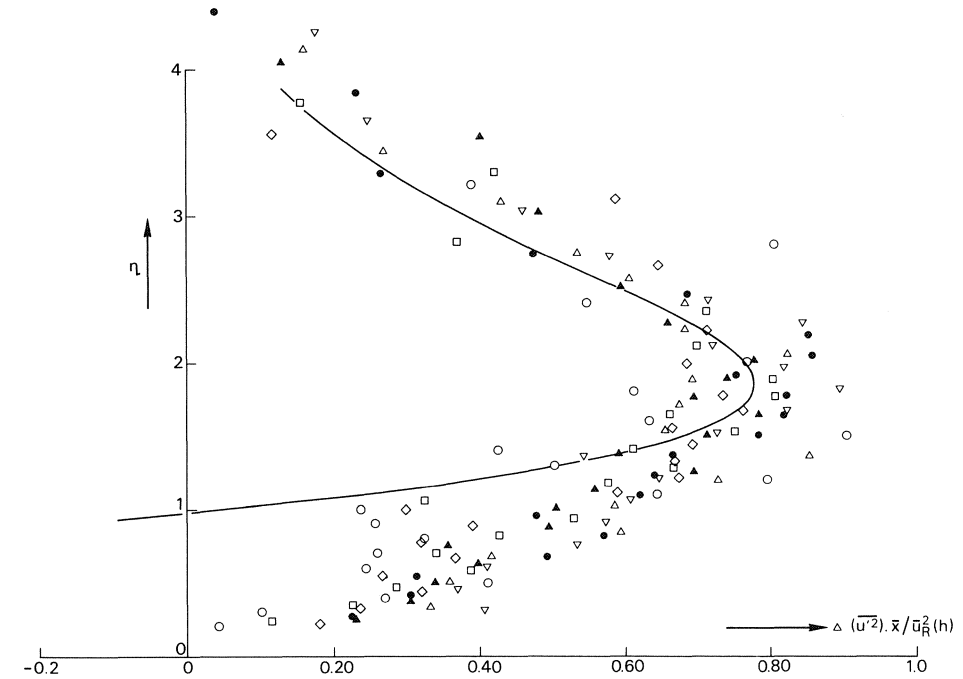

Fig. 7. Excess normal-stress profiles behind solid fence (for key, see Fig. 5(a)).

3.7 Power spectra behind the solid fence

The power spectrum $S(n)$ behind the solid fence was measured with a single-wire HWA probe. Figure 8 shows a set of representative spectra measured at $h/2$ for various distances downstream. The energy $S(n)$ at frequency n has been normalised by the *local* normal stress $\overline{u'^2}$, and is plotted against

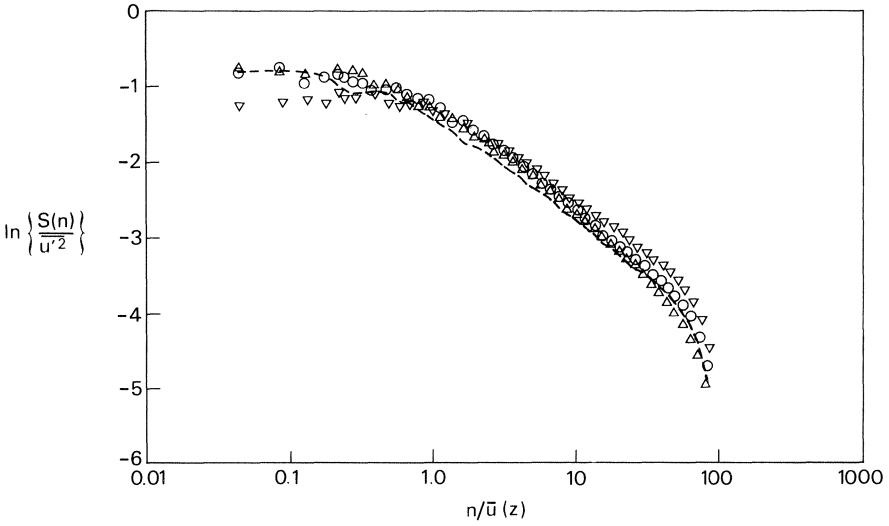

– – – – – – – Reference, x/h = -1.88 (○), 1.25 (△), 3.75 (▽)

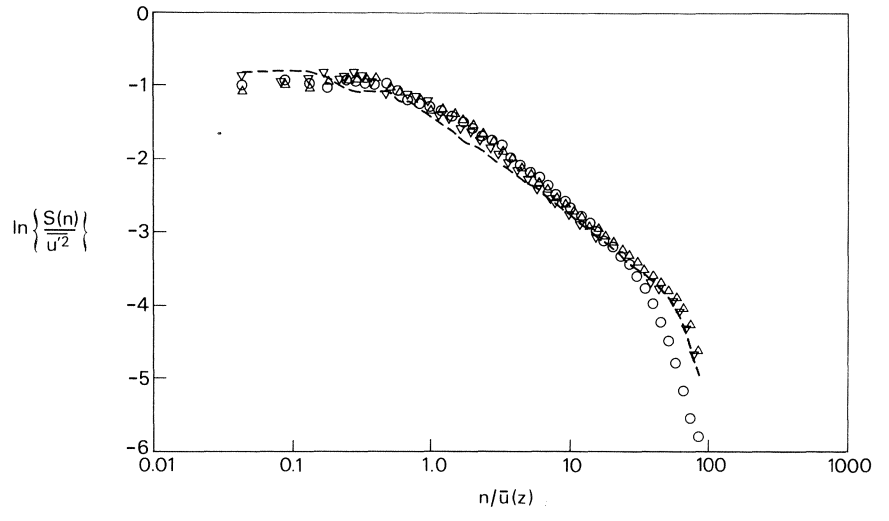

– – – – – – Reference, x/h = - 10 (○), 12.5 (△), 20 (▽)

Fig. 8. Spectra of longitudinal turbulence for solid fence.

the modified frequency $n' = n/\bar{u}(z)$, where n' is a wavenumber only for the reference spectrum.

Although spectra measured in the immediate vicinity of the fence are prone to error, it can be seen that on the whole there are no major differences from the reference spectrum. The only spectrum which does show some deviation is that at $10h$, just past the re-attachment point. All spectra show an inertial subrange with a $-3/2$ decay, unlike the theoretical gradient of $-5/3$. None of the spectra give any indication of large-scale unsteadiness of the wake flow. This contrasts with the findings of Crabb et al. [9] but supports those of Castro [10].

4. Conclusions

If meaningful measurements are to be made in complex flow regions such as fence wakes, then non-rectifying instruments such as pulsed-wire anemometers need to be used.

It is seen that it is the porosity and not the form of construction of the fence that determines the structure of the wake flow. It has been shown that as the porosity of the fence increases, the recirculating bubble detaches from the fence and moves downstream, becoming smaller. Above a porosity of ~ 0.3, the bubble could no longer be detected.

In the far-wake region, it has been shown that mean-velocity defects and excess turbulent stress profiles can be well represented by functional forms. It has been indicated also that both these quantities decay downstream as x^{-1}.

In general, it is difficult to say which value of porosity provides the best shelter. A solid fence is best for protecting the near-wake zone, while a fence with a porosity of 0.1 provides good shelter characteristics in the far wake.

Acknowledgement

The work described herein was carried out as part of the research programme of the Building Research Establishment of the Department of the Environment and is published by permission of the Director.

References

1 J. van Eimern, R. Karschon, L.A. Razumova and G.W. Robertson, Windbreaks and shelterbelts, W.M.O. Tech. Note No. 59 (1964).
2 L.J.S. Bradbury and I.P. Castro, A pulsed-wire technique for velocity measurements in highly turbulent flows, J. Fluid Mech., 49 (1971) 657—691.
3 N.J. Cook, Determination of the model scale factor in wind tunnel simulations of the adiabatic atmospheric boundary layer, J. Ind. Aerodyn., 2 (1977/78) 311—321.
4 J. Counihan, Adiabatic atmospheric boundary layers: a review and analysis of data from the period 1880—1972, Atmos. Environ., 9 (1975) 871—905.
5 I.P. Castro, Wake characteristics of two-dimensional perforated plates normal to an airstream, J. Fluid Mech., 46 (1971) 599—609.

6 J. Gandemer, Wind shelters, Proc. 3rd Colloq. on Industrial Aerodynamics, Aachen, June 1978 (available from Prof. Dr.-Ing. C. Kramer, Fachbereich Flugzeug- und Triebwerkbau der Fachhochschule Aachen, D-5100, Aachen).
7 J. Counihan, J.C.R. Hunt and P.S. Jackson, Wakes behind two-dimensional surface obstacles, J. Fluid Mech., 64 (1974) 529—563.
8 A.A. Townsend, Self-preserving flow inside a turbulent boundary layer, J. Fluid Mech., 22 (1965) 773—797.
9 D. Crabb, D.F.G. Durao and J.H. Whitelaw, Velocity characteristics in the vicinity of a two-dimensional rib, Proc. 4th Brazilian Congr. of Mech. Engs., Florianpolis, 1977, Pap. B-3.
10 I.P. Castro, Relaxing wakes behind surface-mounted obstacles in rough wall boundary layers, J. Fluid Mech., 93 (1979) 631—659.